

## Construction of Ti-Nb-Ti<sub>2</sub>Cu pseudo-ternary phase diagram

Kotaro SATO, Masatoshi TAKAHASHI and Yukyo TAKADA

Division of Dental Biomaterials, Tohoku University Graduate School of Dentistry, 4-1 Seiryomachi, Aoba-ku, Sendai 980-8575, Japan

Corresponding author, Masatoshi TAKAHASHI; E-mail: takahashi@m.tohoku.ac.jp

The aim of this study was to construct a Ti-Nb-Cu ternary phase diagram that plays the role of a map for developing new titanium alloys with excellent machinability and mechanical properties. Fifteen experimental Ti-Nb-Cu ternary alloys composed of Ti-5–30%Nb-2–20%Cu were designed, and ingots made using Ar-arc melting furnace before casting to generate specimen. The alloy castings were evaluated in terms of their microstructures and alloy phases. A Ti-Nb-Ti<sub>2</sub>Cu pseudo-ternary phase diagram was constructed using X-ray diffractometry results. Three alloy phases ( $\alpha$ -Ti,  $\beta$ -Ti and Ti<sub>2</sub>Cu) were established within the specimen. Furthermore, the presence of two-phase coexistence regions ( $\alpha$ +Ti<sub>2</sub>Cu,  $\alpha$ + $\beta$  and  $\beta$ +Ti<sub>2</sub>Cu), and three-phase coexistence region ( $\alpha$ + $\beta$ +Ti<sub>2</sub>Cu) was noted. The findings obtained through microstructural observation corresponded well with the constructed phase diagram.

**Keywords:** Ti-Nb-Cu alloy, Ternary phase diagram, X-ray diffraction, Microstructure, Titanium alloy

### INTRODUCTION

Titanium is a well known material for good biocompatibility and excellent corrosion resistance, thus widely used for dental implants and metal base dentures. However, the strength of titanium is not adequate for dental prostheses which need relatively high strength such as long span bridges and narrow-diameter dental implants<sup>1,2</sup>. Conventional titanium alloys such as Ti-6Al-4V and Ti-6Al-7Nb have higher strength compared to pure titanium, although their machinability is very poor<sup>3</sup>. Since Titanium, Ti-6Al-4V or Ti-6Al-7Nb are difficult-to-machine, making adjustments or polishing of dental prostheses is difficult. Currently, significant and fast evolution is taking place in dental CAD/CAM systems, that would make it possible for metallic dental prostheses be made using dental CAD/CAM in the near future in spite of the known difficulty in processing titanium using CAD/CAM<sup>4</sup>. Improved machinability of titanium is still a highly desirable quality, in addition to the special cutting tool for titanium and its alloys that has already been developed<sup>5</sup>.

Several binary titanium alloys like Ti-Nb and Ti-Cu alloys have been developed aiming at good mechanical and machinability properties and their properties further investigated<sup>6</sup>. Some compositions of Ti-Nb and Ti-Cu alloys showed an improvement in both properties. Tensile strength and yield strength of Ti-Nb alloys with 2–30 mass%Nb (hereafter, “%” stands for “mass%”) were found to be significantly higher than those of Ti. Additionally, the grindability (*i.e.*, the ease of grinding) of Ti-30%Nb alloys was notably higher than that of Ti at low grinding speeds<sup>7</sup>. The solid-solution strengthening of the  $\beta$ -phase and the precipitation of metastable phase “ $\omega$ ” probably contributed to improved strength and grindability properties of Ti-30%Nb<sup>7</sup>. Notably, the tensile and yield strengths of Ti-Cu alloys surpassed those of Ti as the concentration of Cu increased<sup>8</sup>. Furthermore, the high speed grindability of both Ti-5%Cu and Ti-

10%Cu alloys was significantly higher than that of Ti<sup>9</sup>. The solid-solution strengthening of the  $\alpha$ -phase and the precipitation of the microscopic intermetallic compound “Ti<sub>2</sub>Cu” was most likely responsible for the improved characteristics of Ti-5%Cu and Ti-10%Cu alloys.

The existence of secondary phases in the matrix such as  $\omega$ -phase or Ti<sub>2</sub>Cu, seems to contribute to higher strength and hardness<sup>6</sup>. Alloys with favorable grindability have decreased elongation and contain secondary phase<sup>6</sup>. The precipitated secondary phase may act as a local brittle zone similar to the concept of inclusions in free-machining materials<sup>10</sup>. This hypothesis is also applicable in the case of Ti-Ag alloys<sup>4,11</sup> and Ti-Zr alloys<sup>12</sup>. Ternary titanium alloys which are a combination of binary Ti-Nb and Ti-Cu alloys, may exhibit higher strength and better grindability. Based on the equilibrium phase diagram for the Ti-Nb system<sup>13</sup> and that of the Ti-Cu system<sup>14</sup>, various alloy phases such as:  $\alpha$ + $\beta$ ,  $\alpha$ +Ti<sub>2</sub>Cu,  $\beta$ +Ti<sub>2</sub>Cu and  $\alpha$ + $\beta$ +Ti<sub>2</sub>Cu appear to exist in Ti-Nb-Cu alloys. In a recent study, Takahashi *et al.* investigated three kinds of experimental Ti-Nb-Cu alloys and found that the Ti-18%Nb-2%Cu alloy was an  $\alpha$ + $\beta$  type alloy with high strength<sup>15</sup>.

Alloying of metals changes their phases and structures. These changes in the metal structure influence properties such as: strength, elongation, hardness and grindability. Therefore, a phase diagram is an indispensable aspect of alloy design during the development and study stages of any new alloy. Most of the phase diagrams for binary titanium alloys are known<sup>16,17</sup>. However, many phase diagrams for ternary titanium alloys have not been revealed, because there are numerous combinations of any three elements possible. The phase diagrams of ternary Ti-Nb-Cu alloys which are of interest in this study, are unreported. Thus, priority was given to investigation and detailed study of the alloy phases and microstructures that exist in ternary Ti-Nb-Cu alloys. Any phase diagram changes depending on the cooling rate. Since the specimen to

be used in this study are fabricated through casting; the phase diagrams were constructed under conditions applicable for dental casting.

In the present study, ternary Ti-Nb-Cu alloys of various compositions were designed, and alloy ingots prepared. The alloy castings were evaluated in terms of their microstructures and alloy phases. Ti-Nb-Cu ternary phase diagrams were constructed and the composition range suitable for dental applications identified.

## MATERIALS AND METHODS

### *Alloy design*

Fifteen different kinds of compositions of experimental ternary Ti-Nb-Cu alloys were derived from combination

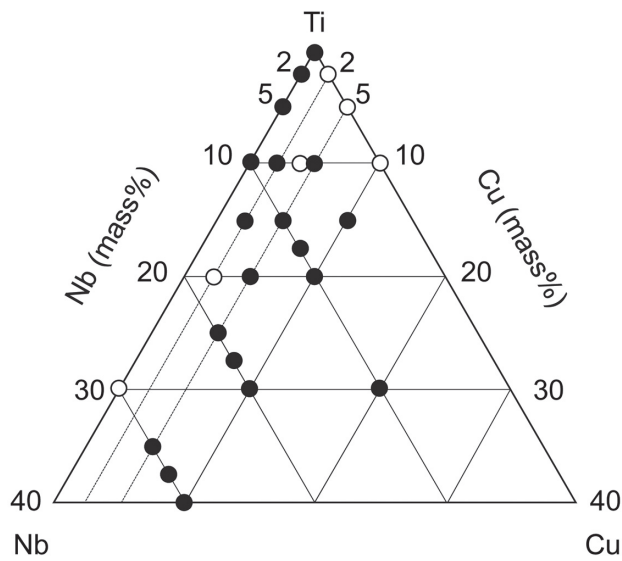


Fig. 1 Compositions of ternary Ti-Nb-Cu alloys.

of base binary alloys: Ti-Nb alloys and Ti-Cu alloys. Black dots in Fig. 1 show the various alloy compositions investigated in this study whereas white dots show compositions investigated in previous studies<sup>7,15</sup>. Compositions of experimental ternary titanium alloys were determined according to the following guidelines. The alloy phases of Ti-Nb alloys shows changes at composition of 10%Nb, 20%Nb, 30%Nb whereas those of Ti-Cu alloys do at 5%Cu, 7.5%Cu, 10%Cu. These compositions were combined and nine possible kinds of the ternary alloys, which are summarized in Table 1, were derived. The different compositions attained are as follows: Ti-10%Nb-5%Cu (10Nb5Cu), Ti-10%Nb-7.5%Cu (10Nb7.5Cu), Ti-10%Nb-10%Cu (10Nb10Cu), Ti-20%Nb-5%Cu (20Nb5Cu), Ti-20%Nb-7.5%Cu (20Nb7.5Cu), Ti-20%Nb-10%Cu (20Nb10Cu), Ti-30%Nb-5%Cu (30Nb5Cu), Ti-30%Nb-7.5%Cu (30Nb7.5Cu) and Ti-30%Nb-10%Cu (30Nb10Cu). Besides, 2%Cu, 5%Cu and 10%Cu in binary Ti-Cu alloys whose mechanical properties and grindability have previously been studied in details<sup>9,10</sup>, were also considered for incorporation in designing of the experimental ternary alloys used in this study. The percentage amount of Nb to be added to the various Ti-Cu alloys was calculated so that the total amount of Nb and Cu elements would make up 10, 15 and 20% of the experimental ternary alloy. The outcome lead to five different kinds of the ternary alloys: Ti-8%Nb-2%Cu (8Nb2Cu), Ti-13%Nb-2%Cu (13Nb2Cu), Ti-5%Nb-5%Cu (5Nb5Cu), Ti-15%Nb-5%Cu (15Nb5Cu) and Ti-5%Nb-10%Cu (5Nb10Cu) as summarized in Table 2. Furthermore, Ti-10%Nb-20%Cu (10Nb20Cu) one of the Cu-rich compositions of the experimental ternary Ti-Nb-Cu alloys was selected for detailed study of alloy phases. In addition, three binary alloys: Ti-2%Nb, Ti-5%Nb and Ti-10%Nb which have been evaluated and reported in a previous study<sup>8</sup>) were considered for further examination of their alloy phases.

Table 1 Composition and abbreviations of the Ti-Nb-Cu alloys (part 1)

		Amount of Nb		
		10%Nb	20%Nb	30%Nb
Amount of Cu	5%Cu	10Nb5Cu	20Nb5Cu	30Nb5Cu
	7.5%Cu	10Nb7.5Cu	20Nb7.5Cu	30Nb7.5Cu
	10%Cu	10Nb10Cu	20Nb10Cu	30Nb10Cu

Table 2 Composition and abbreviations of the Ti-Nb-Cu alloys (part 2)

		Total amount of addition elements		
		10%	15%	20%
Amount of Cu	2%Cu	8Nb2Cu	13Nb2Cu	*18Nb2Cu
	5%Cu	5Nb5Cu	*10Nb5Cu	15Nb5Cu
	10%Cu	*10Cu	5Nb10Cu	*10Nb10Cu

\*overlap with Table 1 or previous studies data<sup>9,15</sup>

### Preparation of specimens

The desired amounts of Ti sponge (>99.8%, grade S-90, Osaka Titanium Technologies, Amagasaki, Japan), Nb (>99.9%, H.C. Starck, Goslar, Germany), and Cu (>99.99%, Research Institute for Electric and Magnetic Materials, Sendai, Japan) were melted in an Ar-arc melting furnace (TAM-4S, Tachibana Riko, Sendai, Japan) to form a 30 g ingot for each alloy, as was done in a previous study<sup>15)</sup>. The ingots of each Ti-Nb-Cu alloy were cast into test specimens using a magnesia investment (Symbion-TC, i-Cast, Kyoto, Japan) in an Ar gas-pressure dental casting machine (Autocast HC-III, GC, Tokyo, Japan) at 200°C and then bench-cooled. The resultant specimen were 4×11×30 mm slabs. All the cast slabs were abraded to a depth of 300 µm using 180–800 grit SiC papers, in order to remove the hardened surface layer. Afterwards, the slabs were cut into square specimen of 10×10 mm then embedded in epoxy resin (EpoFix, Struers, dallerup, Denmark). Cast Ti-Nb alloys specimens were also prepared in a similar manner.

### X-ray diffractometry

XRD analysis was performed at room temperature using Cu K $\alpha$  radiation generated at 30 kV and 10 mA in an X-ray diffractometer (D2 PHASER, Bruker AXS, Tokyo, Japan). Measurements were carried out over the 2 $\theta$  range of 30–80° with a scanning step width of 0.03°. The Crystallography Open Database (COD) was used for phase identification.

### Metallography

The specimen surfaces were polished using water-based diamond suspensions of particle sizes: 15, 6, 3 and 1 µm then etched with an etching solution (HF:HNO<sub>3</sub>:H<sub>2</sub>O=1:4:25). The etched surfaces were examined using an optical microscope (PMG3-614U, Olympus, Tokyo, Japan). Backscattered electron images (composition images) were obtained using a scanning

electron microscopy/energy dispersive X-ray analysis (SEM/EDX; JSM-6060, JEOL, Tokyo, Japan). Qualitative and quantitative analysis of selected specimens was also done using the SEM/EDX.

## RESULTS

### X-ray diffractometry

The XRD patterns of the selected Ti-Nb-Cu alloys are shown in Fig. 2 whereas alloy phases identified by XRD are summarized in Table 3. The peaks in the XRD patterns for the Ti-Nb-Cu alloys matched well with those of  $\alpha$ -Ti,  $\beta$ -Ti, and Ti<sub>2</sub>Cu. The presence of the  $\omega$ -phase could not be confirmed. The alloy phases in 5Nb5Cu, 5Nb10Cu, and 10Nb5Cu were  $\alpha$ +Ti<sub>2</sub>Cu. The alloy phases

Table 3 Alloy phases in Ti-Nb-Cu alloys identified by XRD

Composition	Alloy phases
Ti-10%Nb-5%Cu	$\alpha$ +Ti <sub>2</sub> Cu
Ti-10%Nb-7.5%Cu	$\alpha$ + $\beta$ +Ti <sub>2</sub> Cu
Ti-10%Nb-10%Cu	$\alpha$ + $\beta$ +Ti <sub>2</sub> Cu
Ti-20%Nb-5%Cu	$\alpha$ + $\beta$
Ti-20%Nb-7.5%Cu	$\alpha$ + $\beta$ +Ti <sub>2</sub> Cu
Ti-20%Nb-10%Cu	$\alpha$ + $\beta$ +Ti <sub>2</sub> Cu
Ti-30%Nb-5%Cu	$\beta$
Ti-30%Nb-7.5%Cu	$\beta$ +Ti <sub>2</sub> Cu
Ti-30%Nb-10%Cu	$\beta$ +Ti <sub>2</sub> Cu
Ti-8%Nb-2%Cu	$\alpha$ + $\beta$
Ti-5%Nb-5%Cu	$\alpha$ +Ti <sub>2</sub> Cu
Ti-13%Nb-2%Cu	$\alpha$ + $\beta$
Ti-5%Nb-10%Cu	$\alpha$ +Ti <sub>2</sub> Cu
Ti-15%Nb-5%Cu	$\alpha$ + $\beta$
Ti-10%Nb-20%Cu	$\alpha$ + $\beta$ +Ti <sub>2</sub> Cu

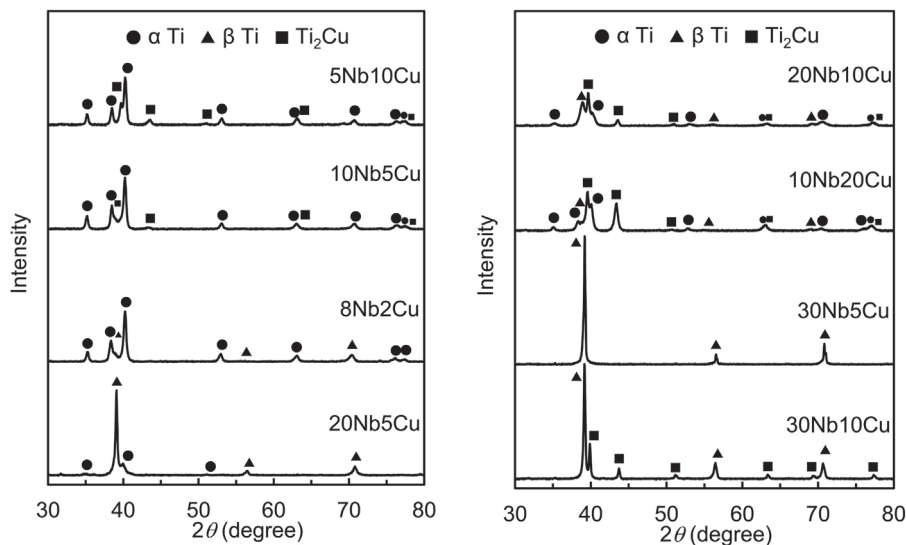


Fig. 2 X-ray diffraction patterns of ternary Ti-Nb-Cu alloys.



in 8Nb2Cu, 13Nb2Cu, 15Nb5Cu and 20Nb5Cu were  $\alpha+\beta$ . 10Nb7.5Cu, 10Nb10Cu, 20Nb7.5Cu, 20Nb10Cu and 10Nb20Cu had  $\alpha+\beta+\text{Ti}_2\text{Cu}$  alloy phases. The alloy phase in 30Nb5Cu was single  $\beta$  whereas 30Nb7.5Cu and 30Nb10Cu showed  $\beta+\text{Ti}_2\text{Cu}$ . For binary Ti-Nb alloys; 2%Nb and 5%Nb showed single  $\alpha$  alloy phases as 10%Nb showed  $\alpha+\beta$ .

#### Metallography

Typical microstructures identified by XRD in the Ti-Nb-Cu alloys showing the five types alloy phases ( $\alpha+\text{Ti}_2\text{Cu}$ ,  $\alpha+\beta$ ,  $\alpha+\beta+\text{Ti}_2\text{Cu}$ , single  $\beta$ , and  $\beta+\text{Ti}_2\text{Cu}$ ) are shown in Fig. 3. Dendritic structures which are characteristic of casting, were observed in all the compositions. In the 5Nb10Cu and 10Nb5Cu alloy specimens which showed  $\alpha+\text{Ti}_2\text{Cu}$  phases; acicular structures, characteristic of  $\alpha$ -Ti, were consistently observed on the entire surface. Backscattered electron images of the 5Nb10Cu and 10Nb5Cu alloy specimens are shown in Fig. 4. Trace amounts of  $\text{Ti}_2\text{Cu}$  intermetallic compounds, were

precipitated within the grains and grain boundaries. The concentration of Cu present in the precipitated  $\text{Ti}_2\text{Cu}$  was significantly higher than that of the  $\alpha$ -Ti matrix. 5Nb10Cu contained higher amounts of  $\text{Ti}_2\text{Cu}$  than 10Nb5Cu. In the 8Nb2Cu alloy whose phases were  $\alpha+\beta$ ; acicular structures of  $\alpha$  were spread throughout the entire surface in comparison to the equiaxed grains of  $\beta$  which were scanty. On the other hand, 20Nb5Cu alloy whose phases were also  $\alpha+\beta$ ; precipitated fine, acicular  $\alpha$  phase observed sparingly in the equiaxed  $\beta$  grains and grain boundaries. Neither  $\text{Ti}_2\text{Cu}$  nor areas of Cu high concentration were found in 8Nb2Cu and 20Nb5Cu alloy specimens. 20Nb10Cu alloy specimen whose phases were  $\alpha+\beta+\text{Ti}_2\text{Cu}$ ; acicular structures of  $\alpha$  and  $\text{Ti}_2\text{Cu}$  phases were found in the  $\beta$  grains. In the alloy 10Nb20Cu whose alloy phases were also  $\alpha+\beta+\text{Ti}_2\text{Cu}$ ;  $\beta$  grains were enclosed by  $\text{Ti}_2\text{Cu}$ , and fine acicular structures of  $\alpha$  and  $\text{Ti}_2\text{Cu}$  precipitated in the  $\beta$  grains. 30Nb5Cu alloy specimens with a single  $\beta$  phase showed equiaxed structures characteristic of  $\beta$ -Ti consistently

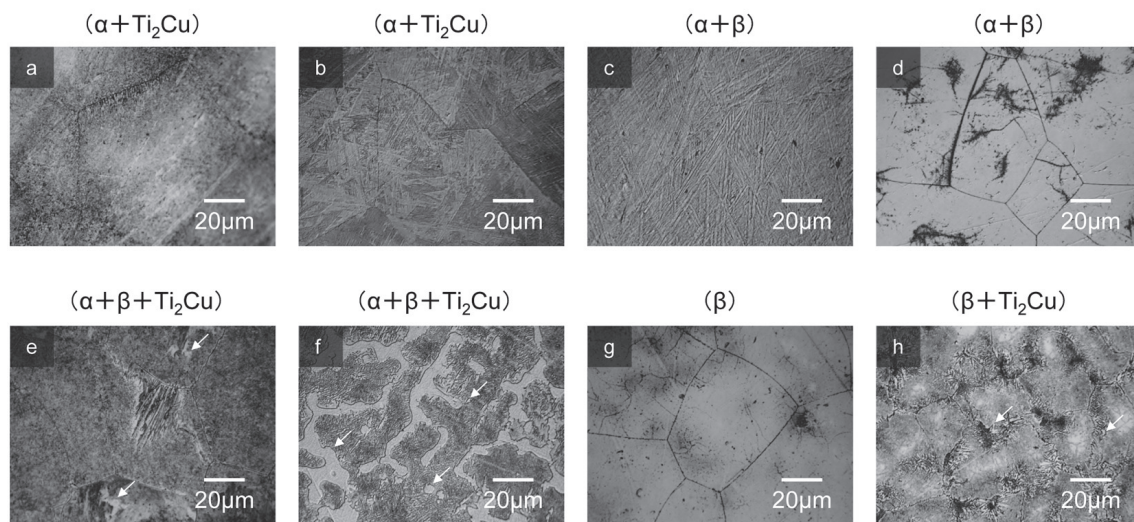


Fig. 3 Microstructures of the etched Ti-Nb-Cu alloys: (a) Ti-5Nb-10Cu, (b) Ti-10Nb-5Cu, (c) Ti-8Nb-2Cu, (d) Ti-20Nb-5Cu, (e) Ti-20Nb-10Cu, (f) Ti-10Nb-20Cu, (g) Ti-30Nb-5Cu, and (h) Ti-30Nb-10Cu. The arrows indicate  $\text{Ti}_2\text{Cu}$ .

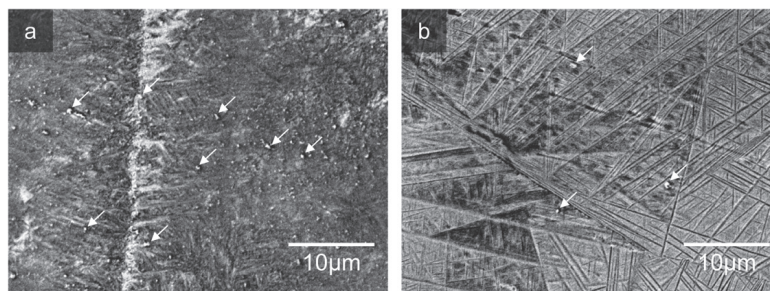


Fig. 4 Backscattered electron images of the Ti-Nb-Cu alloys: (a) Ti-5Nb-10Cu and (b) Ti-10Nb-5Cu. The arrows indicate  $\text{Ti}_2\text{Cu}$ .

spread out through the entire surface. In the 30Nb10Cu alloy specimen whose phases were  $\beta$ +Ti<sub>2</sub>Cu; Ti<sub>2</sub>Cu was found within the  $\beta$  grains and grain boundaries.

## DISCUSSION

### Ti-Nb-Ti<sub>2</sub>Cu pseudo-ternary phase diagram

Equilibrium binary phase diagram of Ti-Nb system can be described as one with continuous  $\beta$ -phase solid solubility and partial miscibility in the  $\alpha$ -phase (Fig. 5)<sup>13</sup>. The melting point of Ti-Nb alloys rises gently as the concentration of Nb increases. Upon solidification of the melted alloys, a primary crystal ( $\beta$  phase) which is Nb-rich forms. Below the solidus curve, the alloy phase changes to single  $\beta$  phase. As the temperature falls further, a part or whole of  $\beta$  phase transforms to  $\alpha$ . Alloys with Nb concentration of less than 4% are located within the  $\alpha$ -region at 400°C, whereas alloys with Nb concentrations of 4–56% are located within the  $\alpha$ + $\beta$  region. The alloy phases formed as a result of nonequilibrium solidification such as in casting, are not always in agreement with the equilibrium phase diagram. Kikuchi *et al.* examined the alloy phases of dental cast Ti-Nb alloys and reported that alloys with a Nb concentration of up to 10%, 15–25%, and 30%; were  $\alpha$ / $\alpha'$ ,  $\alpha''$ , and  $\beta$ + $\omega$ , respectively<sup>8</sup>. However, it is difficult to distinguish between  $\alpha$ ,  $\alpha'$  and  $\alpha''$  just as it is difficult to identify the  $\omega$  phase through XRD analysis only. From the results of this study and the derived equilibrium phase diagram of Ti-Nb system<sup>13</sup>, it is appropriate to judge and classify dental cast Ti-Nb alloys based on the main constituent phases as follows: the alloys with a Nb concentration of up to 5% are single  $\alpha$ , between 5–10%Nb the alloy phase changes to  $\alpha$ + $\beta$ , and the alloys with Nb of more than 30% are single  $\beta$ .

The Ti-Cu system is described as one that exhibits an eutectoid transformation (Fig. 6)<sup>14</sup>. The melting point of Ti-Cu alloys decreases as the concentration of Cu increases. Solidification of the melted Ti-Cu alloys leads to formation of a Ti-rich  $\beta$  phase as the primary crystal phase. The peritectic point of Ti<sub>2</sub>Cu (39.9%Cu) is at 1,005°C, and the range for the peritectic reaction is 17.2–43.3%Cu. Furthermore, the eutectoid point of  $\alpha$ -Ti and Ti<sub>2</sub>Cu (7.0%Cu) is at 790°C, and the range for the eutectoid reaction is 2.1–39.9%Cu. Most alloy phases of Ti-Cu alloys with a Cu concentration of up to 40% should be  $\alpha$ +Ti<sub>2</sub>Cu, since the solid-solubility limit of Cu in Ti ( $\alpha$  solid solution) is almost 0% at 400°C. However, in the case of nonequilibrium solidification for dental cast Ti-Cu alloys, Takahashi *et al.* reported that the Ti<sub>2</sub>Cu phase was not detected in alloys with 2%Cu but was visible in those with more than 5%Cu<sup>9</sup>. Takada *et al.* also reported that 5%Cu alloy appears to have the  $\alpha$ -Ti phase coexist with a slight amount of an intermediate phase containing supersaturated Cu<sup>18</sup>. Based on the above reports, it is appropriate to judge and categorize alloy phases of the dental cast Ti-Cu alloys as follows: alloys with a Cu concentration of up to 2% are single  $\alpha$ , those with 2–5%Cu precipitate Ti<sub>2</sub>Cu in the  $\alpha$ -Ti phase, and the alloys with more than 5% are  $\alpha$ +Ti<sub>2</sub>Cu. On the

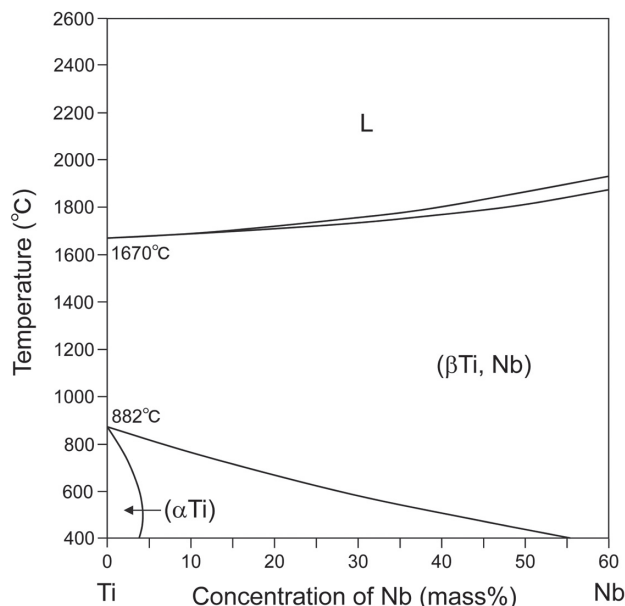


Fig. 5 Equilibrium phase diagram for Ti-Nb system.

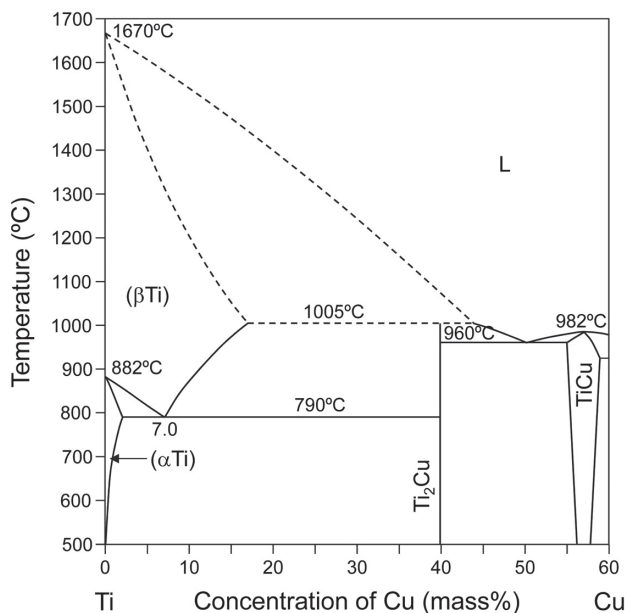


Fig. 6 Equilibrium phase diagram for Ti-Cu system.

other hand, the Cu-Nb system is immiscible, since the solid-solubility limit of Nb in Cu is 0.15% at 1,080°C and the limit of Cu in Nb is 0.8%<sup>19</sup>. In addition, a ternary solid-solution of  $\alpha$  and  $\beta$  phases do exist in the Ti-Nb-Cu system<sup>15</sup>.

Based on the results of this study and data from the references mentioned above, Ti-Nb-Ti<sub>2</sub>Cu pseudo-ternary phase diagram for dental casting at room temperature was constructed (Fig. 7). The black and white dots in Fig. 7 represent data from this current and previous studies, respectively<sup>7,15</sup>. The ternary solid-solution of

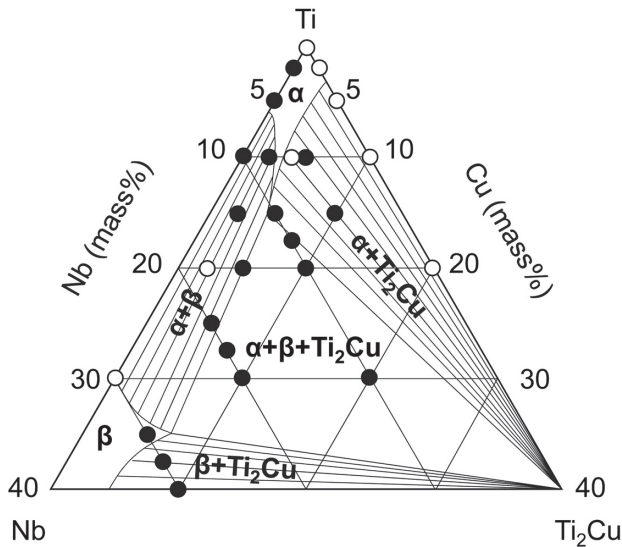


Fig. 7 Ti-Nb-Ti<sub>2</sub>Cu pseudo-ternary phase diagram.

$\alpha$ -Ti,  $\beta$ -Ti and Ti<sub>2</sub>Cu do exist within the compositions examined in this study. Furthermore, three two-phase coexistence regions:  $\alpha$ +Ti<sub>2</sub>Cu,  $\alpha$ + $\beta$  and  $\beta$ +Ti<sub>2</sub>Cu, and one three-phase coexistence region:  $\alpha$ + $\beta$ +Ti<sub>2</sub>Cu do exist. Probably, the composition of  $\alpha$  phase in the three-phase coexistence region of  $\alpha$ + $\beta$ +Ti<sub>2</sub>Cu is almost similar to that of Ti-10%Nb-5%Cu. The composition of  $\beta$  phase in that the region would be known clearly by investigating the alloy phases of Ti-25%Nb-5%Cu and Ti-25%Nb-10%Cu alloys.

#### *Metallography of Ti-Nb-Cu alloys*

Microstructures of  $\alpha$ +Ti<sub>2</sub>Cu alloys showed acicular  $\alpha$  structures and a small amount of precipitated Ti<sub>2</sub>Cu. Compared to 10Nb5Cu and Ti-6%Nb-4%Cu alloys<sup>15)</sup>, 5Nb10Cu alloy contained the highest amount of Ti<sub>2</sub>Cu. These results concur with the  $\alpha$ /Ti<sub>2</sub>Cu ratio which can be obtained from the tie line in the constructed phase diagram (Fig. 7). Microstructures of  $\alpha$ + $\beta$  alloys showed fine acicular  $\alpha$  structures along the  $\beta$  grain boundaries. The amount of  $\alpha$ -phase present in a descending order in alloys of these compositions was: 13Nb2Cu, Ti-18%Nb-2%Cu alloy, and 20Nb5Cu. This order does tally with the  $\alpha$ / $\beta$  ratio which can be obtained from the tie line in the constructed phase diagram (Fig. 7). Acicular  $\alpha$  structures were visible on the entire surface of 8Nb2Cu in spite of  $\alpha$ + $\beta$  being identified by XRD. As shown in the constructed phase diagram of Fig. 7, 8Nb2Cu is probably located at the boundary line between the single  $\alpha$  phase and the  $\alpha$ + $\beta$  region.

Microstructures of the  $\alpha$ + $\beta$ +Ti<sub>2</sub>Cu alloys except 10Nb20Cu, showed precipitated Ti<sub>2</sub>Cu in the grain boundaries and lamella structures in the grains. During casting of the alloys, alloy phases undergo a sequential change;  $L \rightarrow L+\beta \rightarrow \text{single } \beta \rightarrow \beta+\text{Ti}_2\text{Cu} \rightarrow \alpha+\beta+\text{Ti}_2\text{Cu}$ . When the melted alloys begin to solidify, a primary crystal

( $\beta$ ) which is Nb-rich and Cu-lean is formed. As the crystal continues to grow, regions furthest from the center contain relatively more Cu than the center of the grain matrix. The last regions to solidify within the  $\beta$  grains are those adjacent to the grain boundaries. Since the last regions to solidify are also relatively Cu-rich, Ti<sub>2</sub>Cu is inevitably precipitated within the  $\beta$  grain boundaries. Lamella structures are probably produced during the eutectoid reaction of  $\beta\text{-Ti} \rightarrow \alpha\text{-Ti}+\text{Ti}_2\text{Cu}$ . The microstructure of 10Nb20Cu having  $\alpha$ + $\beta$ +Ti<sub>2</sub>Cu alloy phase differed greatly from that of other alloys with  $\alpha$ + $\beta$ +Ti<sub>2</sub>Cu alloy phase, but was similar to that of Ti-20%Cu alloy reported by Takada *et al.*<sup>18)</sup> The microstructural difference can be explained by changes in alloy phases during the solidification process. In the case of 10Nb20Cu, initially, a  $\beta$ -Ti solid-solution is crystallized in the liquid phase during the  $L \rightarrow L+\beta\text{-Ti}$  process. As the temperature reaches the peritectic point,  $\beta$ -Ti dendrites are enclosed with Ti<sub>2</sub>Cu because of the peritectic reaction of  $\beta\text{-Ti}+L \rightarrow \text{Ti}_2\text{Cu}$ . The Ti<sub>2</sub>Cu produced as a result of this reaction is a light-colored structure shown in Fig. 3. Afterwards, the  $\beta$ -Ti changes through  $\beta \rightarrow \beta+\text{Ti}_2\text{Cu} \rightarrow \alpha+\beta+\text{Ti}_2\text{Cu}$  process to produce the final structure including the fine precipitates as shown in Fig. 3. The presence or absence the peritectic reaction leads to the difference in the microstructures of  $\alpha$ + $\beta$ +Ti<sub>2</sub>Cu phase containing alloys.

Microstructure of 30Nb5Cu showed a typical  $\beta$ -Ti structure, while that of 30Nb10Cu showed precipitated Ti<sub>2</sub>Cu in the  $\beta$  grain boundaries. As mentioned above, after 30Nb10Cu alloy phase transits to a single  $\beta$  phase, Ti<sub>2</sub>Cu is precipitated from the regions with high Cu concentration. Furthermore, it was found that  $\beta$  phase of ternary Ti-Nb-Cu alloys can be retained without  $\alpha$  phase by adding 30%Nb, as in the case of binary Ti-Nb alloys also.

#### *Significance of alloy phases in application of dental Ti-Nb-Cu alloys*

The Ti-Nb-Ti<sub>2</sub>Cu pseudo-ternary phase diagram, which had not yet been clarified, was constructed using the results of XRD. Since the phase diagram and the results obtained by microstructural observation correspond well, reliability of the constructed phase diagram is likely to be high. When developing new alloys, the information from phase diagrams is very critical. A phase diagram plays the role of a map, that is useful during design of a new Ti-Nb-Cu alloy. Dental applications suitable for each alloy phase of ternary Ti-Nb-Cu alloys were considered as follows.

Since both  $\alpha$ + $\beta$  titanium alloy and  $\beta$  titanium alloy with high concentration of alloying elements generally show high strength<sup>20)</sup>, the compositions which have these alloy phases are advantageous to devices which needs high strength, such as long span bridges and narrow-diameter dental implants. Moreover, the strength of both  $\alpha$ + $\beta$  titanium alloy and  $\beta$  titanium alloy can be enhanced through heat treatment<sup>20)</sup>. It would be beneficial to further study the toxicity and osseointegration of these alloys which have potential application as implant



materials.

Since  $\beta$ -Ti phase is a body centered cubic structure and exhibits excellent workability<sup>20)</sup>, the compositions of single  $\beta$  phase are advantageous to devices which need considerable elongation. Furthermore, since it is said that the elastic modulus of  $\beta$  titanium alloys is lower than that of  $\alpha$  and  $\alpha+\beta$  titanium alloys<sup>20)</sup>; compositions of single  $\beta$  phase are good for devices in which a low elastic modulus is desired, such as bone plates.

Since a three-phase coexistence region of  $\alpha+\beta+\text{Ti}_2\text{Cu}$  probably has high hardness; the compositions that bear three-phase coexistence are useful for devices which need high wear resistance. Although corrosion resistance of binary Ti-Nb alloys (up to 35%Nb) and Ti-Cu alloys (up to 20%Cu) is as good as that of that of titanium, evaluation of corrosion resistance of these alloys is indispensable because it maybe lower in multiphase alloys compared to single phase ones<sup>21)</sup>.

Since the Nb-rich  $\beta$  phase enhanced low speed grindability<sup>8)</sup> and moderate precipitation of  $\text{Ti}_2\text{Cu}$  enhanced high speed grindability<sup>10)</sup>; compositions that contain  $\beta+\text{Ti}_2\text{Cu}$  may exhibit good grindability at high grinding speeds and/or low grinding speeds. Compositions suitable for CAD/CAM processing should be investigated further because grinding and cutting mechanisms differ.

## ACKNOWLEDGMENTS

The authors are pleased to acknowledge the assistance of Dr. Mary Wambui KANYI in proofreading and editing the English version. This study was partially supported financially by JSPS KAKENHI Grant Number JP18K09633.

## REFERENCES

- 1) ISO 22674, Dentistry –Metallic materials for fixed and removable restorations and appliances. ISO, Switzerland, 2006, pp.1-22.
- 2) Davarpanah M, Martinez H, Tecucianu JF, Celletti R, Lazzara R. Small-diameter implants: indications and contraindications. *J Esthet Dent* 2000; 12: 186-194.
- 3) Kikuchi M, Okuno O. Machinability evaluation of titanium alloys. *Dent Mater J* 2004; 23: 37-45.
- 4) Inagaki R, Kikuchi M, Takahashi M, Takada Y, Sasaki K. Machinability of an experimental Ti-Ag alloy in terms of tool life in a dental CAD/CAM system. *Dent Mater J* 2015; 34: 679-685.
- 5) Kasahara H, Sato H, Kameyama Y, Sato H, Oyaizu Y, Shimpo R, *et al.* Precision polishing of purity titanium and Ti-Ag alloys for dentistry. *J J Soc Abrasive Tech* 2014; 58: 777-778.
- 6) Kikuchi M. Development of titanium alloys for dental CAD/CAM systems. *Kagoshima Univ Repository* 2014; 34: 41-51.
- 7) Kikuchi M, Takahashi M, Okuno O. Mechanical properties and grindability of dental cast Ti-Nb alloys. *Dent Mater J* 2003; 22: 328-342.
- 8) Takahashi M, Kikuchi M, Takada Y, Okuno O. Mechanical properties and microstructures of dental cast Ti-Ag and Ti-Cu alloys. *Dent Mater J* 2002; 21: 270-280.
- 9) Kikuchi M, Takahashi M, Okabe T, Okuno O. Grindability of dental cast Ti-Ag and Ti-Cu alloys. *Dent Mater J* 2003; 22: 191-205.
- 10) Finn ME. Machining of carbon and alloy steels. *Metals Handbook 9th Ed. Vol. 16 Machining*. ASM Int 1989: 666-677.
- 11) Takahashi M, Kikuchi M, Takada Y. Mechanical properties of dental Ti-Ag alloys with 22.5, 25, 27.5, and 30 mass% Ag. *Dent Mater J* 2015; 34: 503-507.
- 12) Takahashi M, Kikuchi M, Okuno O. Grindability of dental cast Ti-Zr alloys. *Mater Trans* 2009; 50: 859-863.
- 13) Joanne LM. Nb-Ti (Niobium-Titanium). *Binary alloy phase diagrams 2nd Ed. Vol. 3*. ASM Int 1990: 2775-2778.
- 14) Joanne LM. Cu-Ti (Copper-Titanium). *Binary alloy phase diagrams 2nd Ed. Vol. 2*. ASM Int 1990: 1494-1496.
- 15) Takahashi M, Kikuchi M, Takada Y. Mechanical properties and microstructures of dental cast Ti-6Nb-4Cu, Ti-18Nb-2Cu, and Ti-24Nb-1Cu alloys. *Dent Mater J* 2016; 35: 564-570.
- 16) Hugh Baker Ed. *ASM Handbook Vol. 3 Alloy phase diagram*. ASM Int 1992.
- 17) Joanne LM Ed. *Phase diagrams of binary titanium alloys*. ASM Int 1987.
- 18) Takada Y, Okuno O. Corrosion characteristics of  $\alpha$ -Ti and  $\text{Ti}_2\text{Cu}$  composing Ti-Cu alloys. *Dent Mater J* 2005; 24: 610-616.
- 19) Chakrabarti DJ, Laughlin DE. Cu-Nb (Copper-Niobium). *Binary alloy phase diagrams 2nd Ed. Vol 2*. ASM Int 1990: 1440-1441.
- 20) Oda Y. Forefront of dental application of titanium. *J Tokyo Dent Coll Soc* 2014; 114: 187-197.
- 21) Noël JJ. Effect of metallurgical variables on aqueous corrosion. *ASM Handbook Vol. 13A Corrosion: fundamentals, testing, and protection*. ASM Int 2003: 258-265.